THE GROUND ACCELERATION OF HISTORICAL EARTHQUAKES

J.R. Arango-González[1]

ABSTRACT

There exists in Spain a body of literature on the subject of historic earthquakes which, due to the lack of adequate analysis of the information available, turns out to be practically worthless.

This article investigates the Andalusian Earthquake (25/12/1884). Ground liquefaction is analyzed at five sites within the province of Granada and Málaga, as well as in the damage caused to the Restábal Church. The final conclusions show the minimum acceleration value, which causes both the ground liquefaction as well as damage to the building itself.

This research's starting point is taken from historic data found in reports carried out by Official Spanish, Italian and French Commissions sent to study the earthquake. Those documents provide us with information about the damage caused both to the buildings themselves, as well as to the effects on the ground.

The geotechnical data needed to check ground liquefaction was obtained by penetration tests. The mechanical characteristics and resistance of the materials of the building, essential for the analysis of their seismic resistance, were taken from samples carried out in the laboratory on the same materials or from already existing data from similar materials.

INTRODUCTION

The Andalusian Earthquake (Figure 1), took place at 21:08 on the 25th of December 1884, its effects extending throughout a large area of the provinces of Granada and Málaga [10, 11]. The research was carried out by an Official Spanish Commission headed by Fernández de Castro [6], together with both an Italian and French Commission headed by Tarramelli and Mercalli [17] and Fouqué [7] respectively.

The Spanish Commission reports describe phenomena interpreted by López et al. [10] as ground liquefaction in the following sites: (1) "Rio Marchán", (2) "Cortijo de los Álamos", (3) "Santa Cruz del Comercio", (4) "Llano de las Donas",(5) " Pago de las Ventas", (6) "Río Bermuza", and (7) "Vélez Málaga" (see Figure 2).

On the other hand, the Spanish Commission refers to the damage caused to churches and the principal buildings of the area, special mention being made of the Restábal Church.

In the first part of this research, the liquefaction potential is analyzed at the following sites: (1), (2), (3), (4), and (6), in order to obtain the minimum value where liquefaction is caused by ground acceleration.

Once the site was chosen and the necessary dynamic penetration test carried out, the ground liquefaction potential was assessed by comparing the value of S.P.T. on each layer of the test sample (Figure 3), which was derived in turn from the dynamic penetration diagrams measured in situ, according to Vanelli and Benassi [20] and Zhou [24], with the N_{crit} value obtained by the norm established by the Chinese State Capital Construction Commission [16].

Once the liquefaction on a ground layer had been checked, the cyclic stress ratio, τ/σ' , and the peak acceleration, A, which would cause its liquefaction, were both calculated according to Seed's simplified procedure [15].

Once the acceleration causing liquefaction in all ground layers of the survey was known, the maximum value of all was assessed, corresponding to the deepest layer. This value, a_{min}, is a limiting value, from which liquefaction in the ground column was found to occur. In other words, the ground acceleration caused by the earthquake on the site was equal or higher to this value a_{min}.

The damage caused by the earthquake was serious, nearly a thousand houses had to be rebuilt and around fourteen thousand restored. The extent of the damage was due, not only to the high magnitude of the earthquake, but also to the low quality of building materials used in their construction.

The seismic response found within the bell tower of Restábal Church allows us to evaluate its seismic resistance, by relating the stresses obtained by the Finite Element Method, F.E.M., in the elastic field to the resistance of the materials in the damaged areas of the bell tower. If we compare the predicted damage

[1] *Department of Civil Engineering, University of Granada, Granada, Spain.*

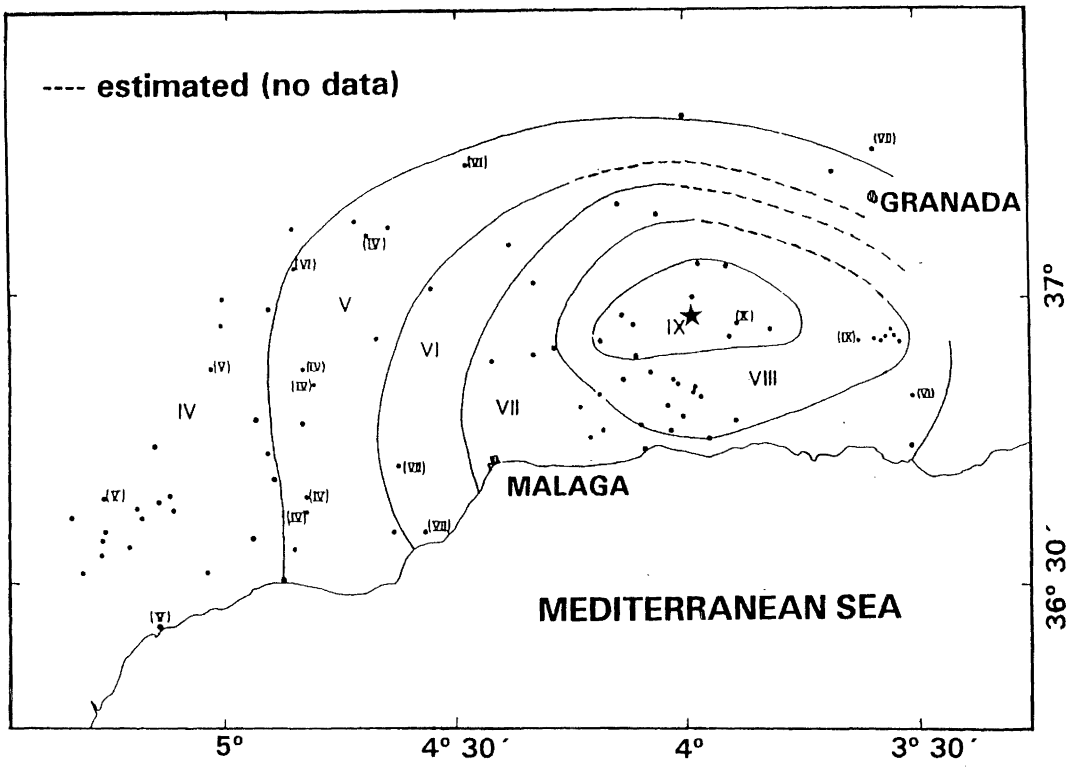

FIGURE 1 Isoseismal map of Andalusian earthquake 12/25/1884 [Muñoz et Udías, 1991].

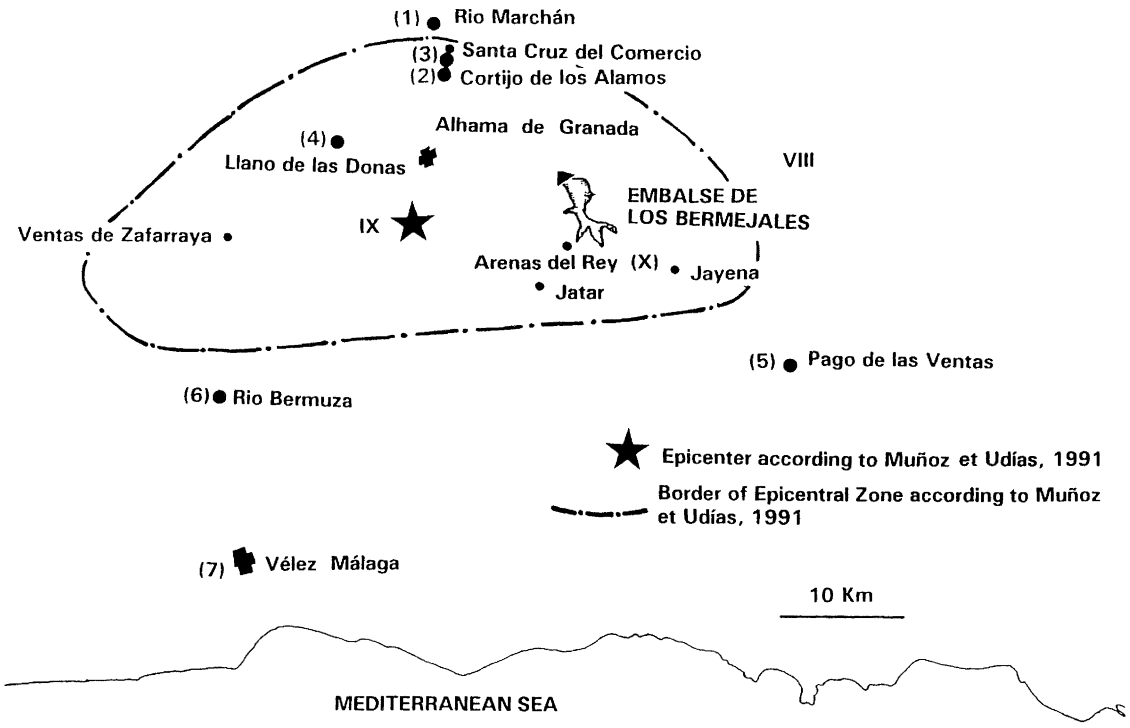

FIGURE 2 Sites where liquefaction presumably occurred

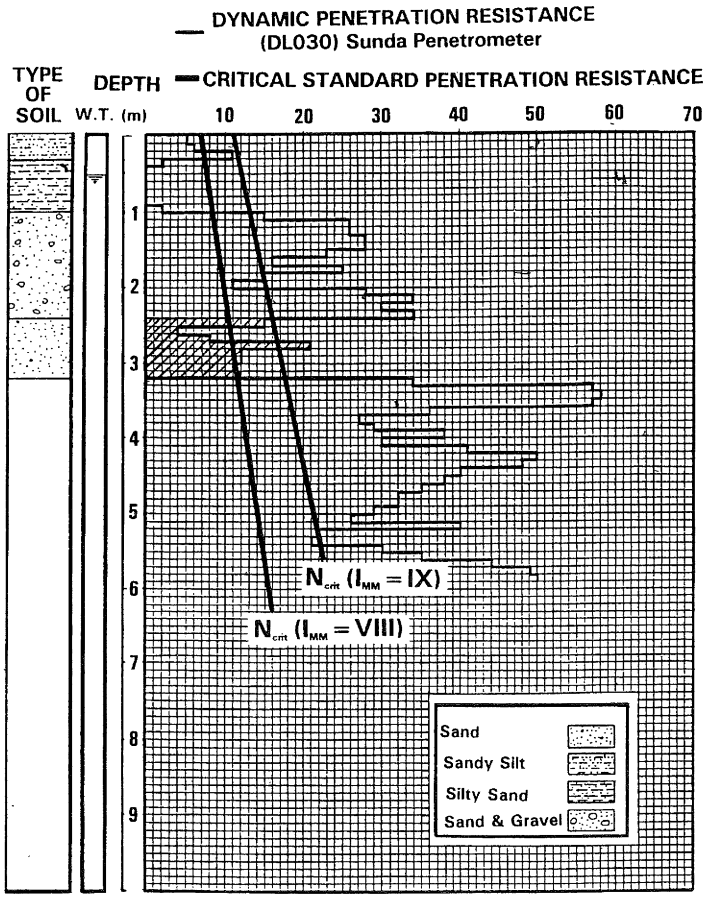

FIGURE 3 Penetration diagram of Rio Marchán (data obtained with DL030 Sunda Penetrometer)

with that caused by the earthquake, i.e., by relating the stresses obtained by the F.E.M. with the material resistance of the damaged areas, we can calculate a minimum value of peak acceleration required to reproduce the damage. The final result produced is represented by the value of the peak acceleration causing wall cracking of the bell tower and the direction of the seismic S waves.

By the above two procedures we can thus estimate the value of the peak acceleration above which ground acceleration in a historic earthquake in a given place, is situated.

GROUND LIQUEFACTION

In order to check the liquefaction potential, the following equation was used.

$$N_{crit} = N[1 + 0.125(d_s - 3) - 0.05(d_w - 2)]$$

It relates both the depth of the sand layer, d_s, in metres, and the depth of the water table, d_w, in metres, with the critical S.P.T. N_{crit}, essential for liquefaction. Critical N values depend on earthquake intensity, I, being N = 16 for I = IX, N = 10 for I = VIII and N = 6 for I = VII.

The earthquake magnitude of 6.6 and the intensity at any of the given sites have been given by Muñoz and Udías [12].

S.P.T. values, the density of the ground layers and the depth in the water table were calculated using penetration samples taken from five of the sites mentioned above. The results of the test are summarized in Table 1.

TABLE 1 Characteristics of soil/profiles

Site	Borehole n°	H	W.T.	Soil	ρ
Valle del rio Marchán	1	0.80	0.60	Silt	1700
	1	2.80	0.60	Sand	2050
Cortijo de los Alamos	1	1.50	1.60	Silt	1700
	2	0.81	0.60	Silt	1810
	1	1.50	0.60	Sand	1910
Santa Cruz del Comercio	1	0.70	0.90	Silt	1800
	1	2.50	0.90	Sand	1920
Llano de las Donas	2	1.50	0.60	Sand	1900
	2	2.90	0.60	Sand	1990
	2	3.70	0.60	Sand	2000
	2	4.50	0.60	Sand	2000
Rio Bermuza	2	2.00	1.20	Sand	1900

H = depth of layer of soil (m)
W.T. = depth of water table (m)
ρ = density of soil (kg/m^3)

For example, Figure 3 shows the penetration diagram in Rio Marchán. Comparing the S.P.T. average value in each layer with N_{crit}, we can infer that the second layer is potentially liquefiable for an earthquake of intensity VIII or IX, as the fourth is for an earthquake with intensity IX.

Liquefaction acceleration

The cyclic stress ratio leading to the liquefaction in a ground layer can be calculated from Figure 4 [15] and the corresponding peak acceleration A in the following equation [15]:

$$\frac{\tau}{\sigma} = 0.65 \frac{A}{g} \frac{\sigma}{\sigma'} r_d$$

The maximum value in all accelerations obtained for a survey, a_{min}, corresponding to the deepest layer, is a limiting value for the ground acceleration from which liquefaction in the whole ground column originates. In other words, the ground acceleration caused by the earthquake had necessarily to be, at least, a_{min}, for ground liquefaction to take place.

In four of the five studied sites, ground liquefaction was confirmed and the following results obtained:

Santa Cruz del Comercio,	a_{min}=0.21g.
El Cortijo de los álamos,	a_{min}=0.23g.
El Llano de las Donas,	a_{min}=0.26g.
Río Bermuza,	a_{min}=0.15g.

Figure 5 shows the above acceleration values obtained, and the epicentre situation (36.95°N, 3.98°W) according to Muñoz and Udías [12].

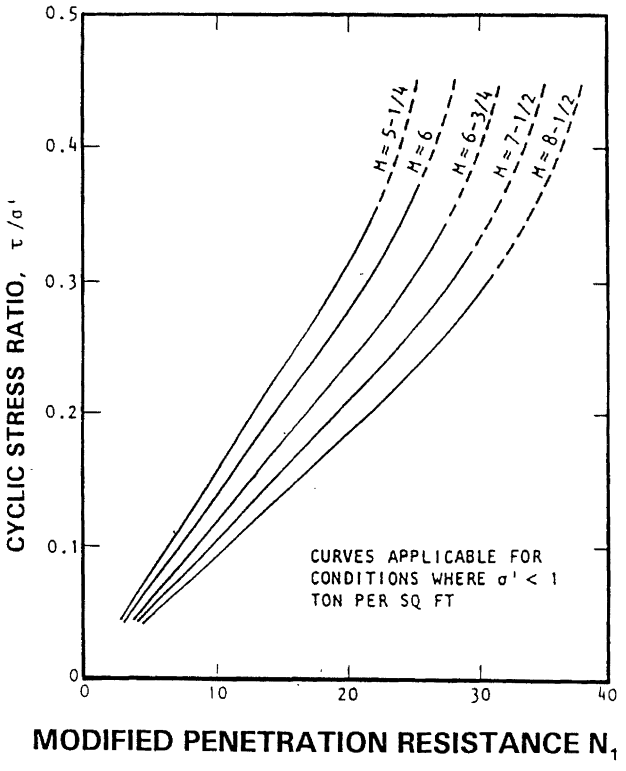

FIGURE 4 Chart for evaluation of liquefaction potential for sands for different magnitude earthquakes [Seed and Idriss, 1982]

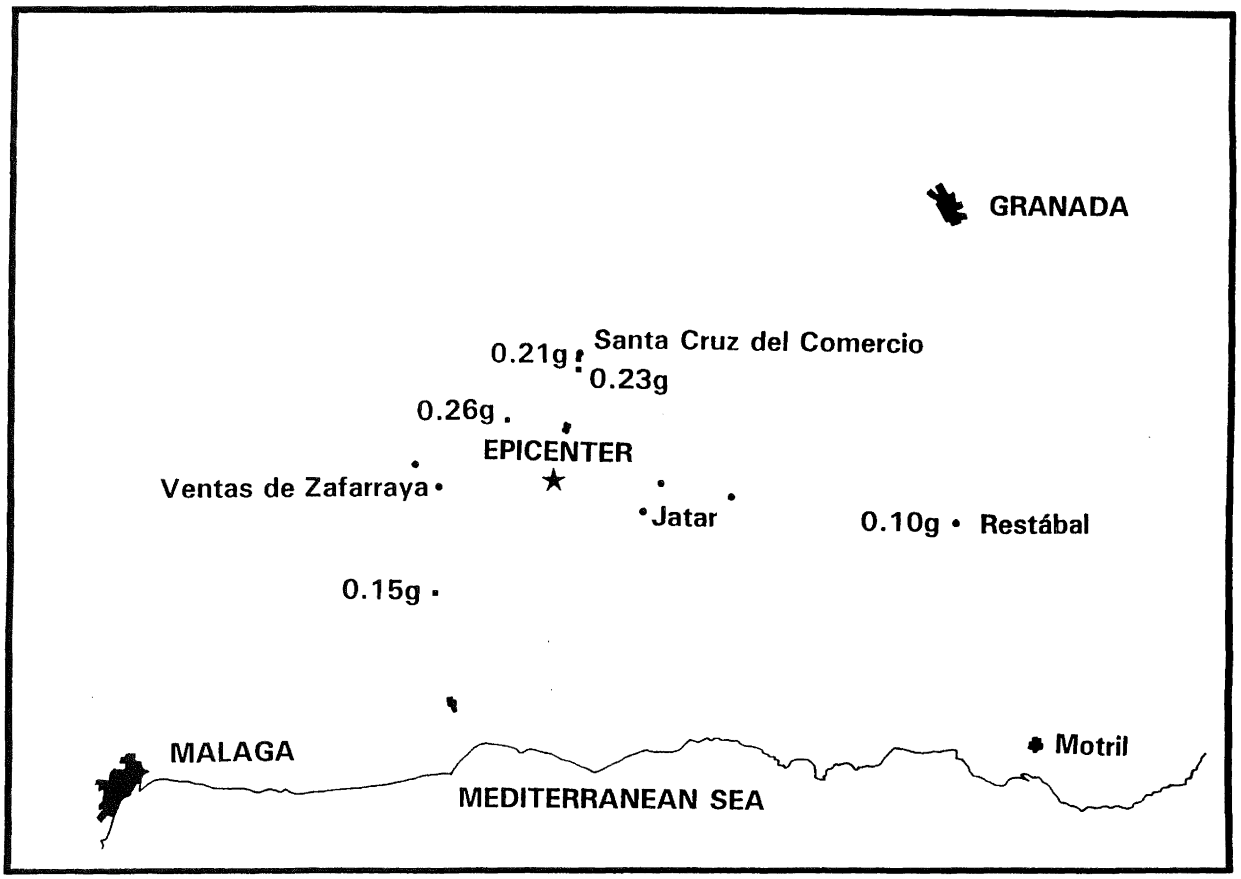

FIGURE 5 Acceleration values obtained and epicentre situation according to Muñoz et Udías [1991].

SEISMIC RESISTANCE OF RESTABAL CHURCH

The walls of Restábal Church were built with brick masonry, being a resistant material, and limestone and dolomite gravel masonry, as stuffing material, both agglomerated by 1:3 lime mortar.

Figure 6 shows the prominent cracks taken from the most fissured wall in the church's bell tower.

Mechanical behaviour of the masonry

Those tests carried out on unreinforced masonry walls, subjected to a combination of vertical and horizontal in-plane forces, reveal shear failure which is characterized with diagonal cracks in the wall, caused by the principal tensile stresses in the wall exceeding the tensile strength of masonry, f_t. For an elastic, homogeneous and isotropic material, the average shear stress in the horizontal cross-section of the wall when this failure [19] occurs is:

$$\tau_u = \frac{f_t}{b}\sqrt{\frac{\sigma_0}{f_t+1}}$$

Where, σ_0 , is the average compressive stress in the horizontal cross-section of the wall due to the vertical load. Factor b determining the distribution of shear stress in the horizontal cross-sectional area of the wall, takes the value 1.0 in the case of a squat wall (height to width ratio equal to 1.0) and the value 1.5 for slender walls (height to width ratio greater than 1.5)

The behaviour of masonry walls when they are loaded out-of-plane, corresponds to the linear relation stress-deformation and to Navier's hypothesis, according to Yokel and Dickers [23] and Benedetti et al. [2].

Considering the mechanical behaviour of masonry, the linear-elastic analysis is preferred instead of nonlinear dynamics; more specifically the M.E.F. was adopted in this research.

Mechanical characteristics and strengths in masonry walls of Restabal Church

Three masonry panels were built with solid bricks that dated from the time of the earthquake, and a 1:3 lime mortar, reproducing the way the building was constructed. The three panels were cured for 28 days at 25° C and at a humidity of 50%.

TABLE 2 Average tensile and compressive strength of bricks water absorption in 24 hour - Restabal Church

Samples	Flexural tensile strength (MPa)	Compressive strength (MPa)	Water absorption %
V, VI	6.20	12.60	10.60

Note : MPa (Megapascal) = 10 kg/cm^2

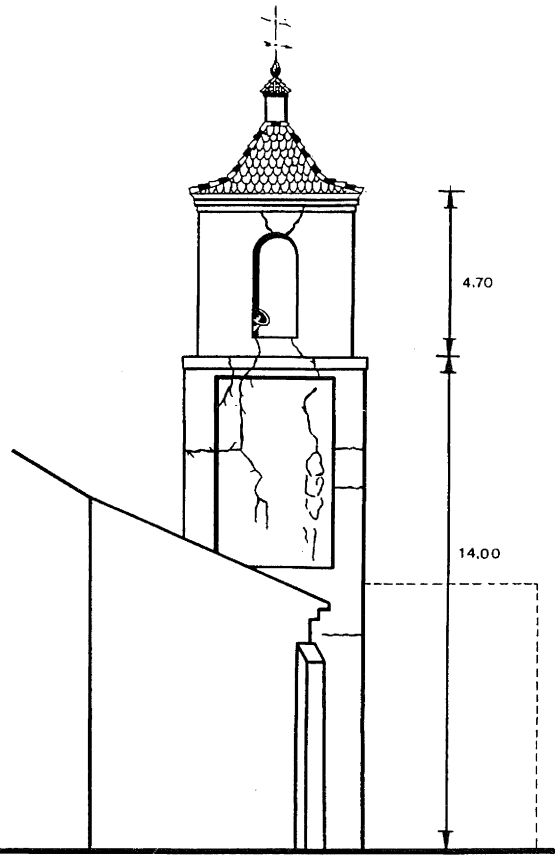

FIGURE 6 Prominent cracks from the most fissured wall, in Figure 7, view 1, in the Restábal church bell tower.

TABLE 3 Mechanical characteristics of brick masonry Restabal Church

Characteristic	Average value
Compressive strength	3.71 (MPa)
Modulus of elasticity	3710.00 (MPa)
Compressive strength of mortar	1.05 (MPa)
Tensile strength of mortar	0.55 (MPa)
Density of brick masonry	1600.00 (kg/m^3)

Note : MPa (Megapascal) = 10 kg/cm^2

The results of the tests carried out with solid bricks, mortar and masonry panels are summarized in Tables 2 and 3.

The remaining mechanical characteristics and resistance of the brick and stone masonry were obtained out from existing data for similar materials. The value of 0.25 MPa (1 Mpa = 10 kg/cm$^{2)}$, was adopted for tensile strength and shear strength of brick masonry, according to those values recommended by Commission of the European Communities [5] for mortar and similar brickwork and the value of 0.20 for the Poisson coefficient was estimated from the works on such material of Page [13] and Atkinson et al. [1].

For the stone masonry, the following values from Tomazevic et al. [18] were adopted: modulus of elasticity, 1000 MPa, tensile strength, 0.15 MPa, and compressive strength, 0.90 MPa. The shear strength was estimated at 0.10 MPa, close to values found in Benedetti and Benzoni [2] and Benedetti et al. [3]. The Poisson coefficient was estimated at 0.30 from the works on such material [14]. The density, 1600 kg/m^3, was evaluated from specimens built for this purpose.

Seismic Resistance

The computer program, SAP80 [21], with 3D shell type elements was adopted for this research. The nodes defining the foundations were considered to be embedded. Figures 7 and 8 show the mesh of finite elements corresponding to the church and the bell tower. It can be seen that those elements belonging to the rectory during the earthquake period, now recently demolished, are shown as discontinuous lines.

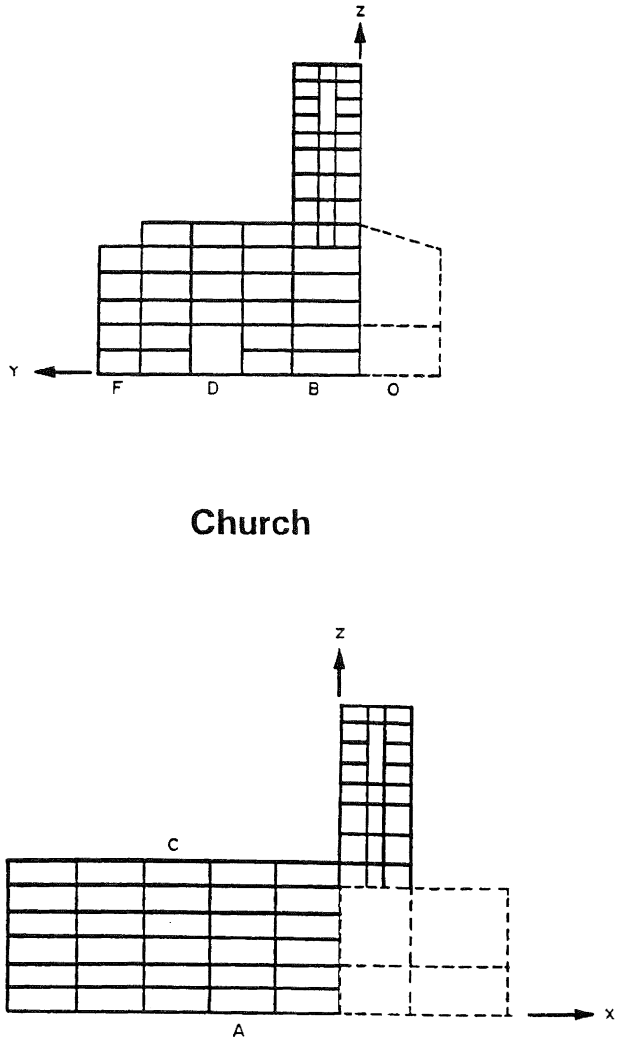

FIGURE 7 Mesh of finite elements for Restábal church.

The seismic input adopted was the response spectrum for rock as shown by Seed [15], since the building is cemented on this material, with a damping of 5% which is a normal value for masonry and was taken from works on similar materials by Ghobarah et al. [9] among other authors.

In each of the possible arrival directions for seismic waves, the tensions obtained in the mesh elements are proportional to the value of the peak acceleration used. Therefore, given a certain arrival direction of the S waves, the peak acceleration cracking the material in the bell tower walls is proportional to the peak acceleration used:

$$r = \frac{acceleration\ causing\ cracking}{peak\ acceleration\ of\ input}$$

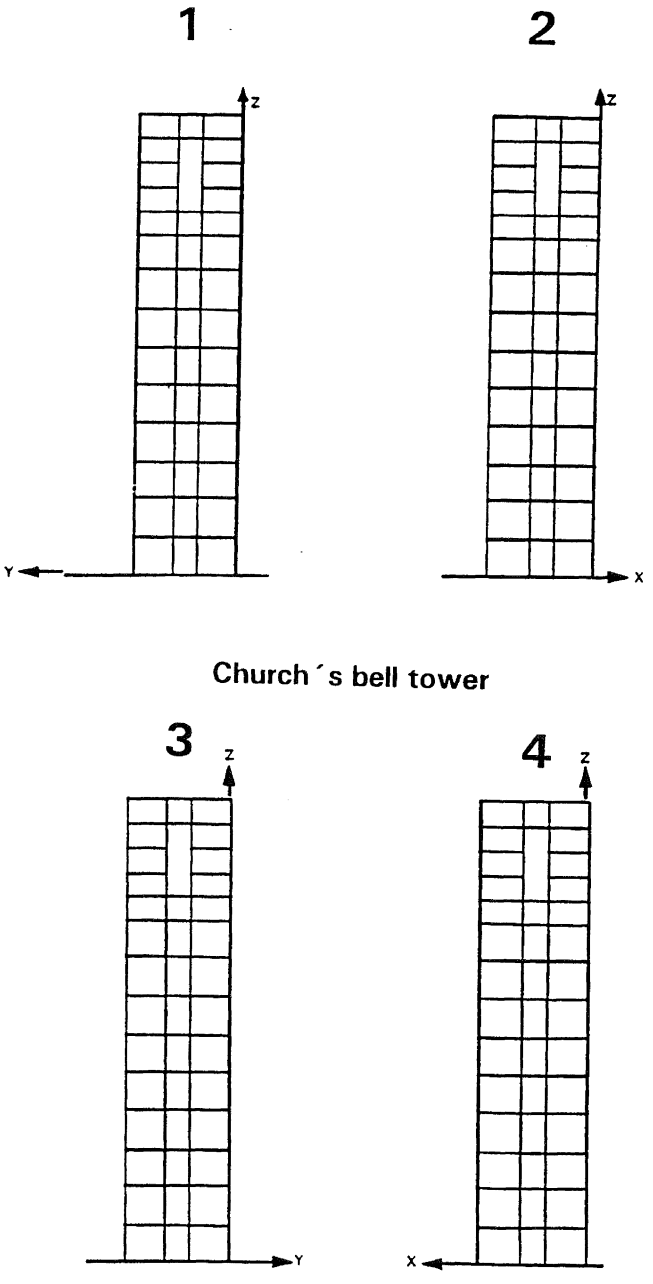

FIGURE 8 Mesh of finite elements for Restábal church bell tower.

The proportionality ratio, r, is the quotient between the cracking strength of the material and the stress obtained in the dynamic calculation, equation 1.

$$r = \frac{cracking\ stress}{stress\ predicted\ by\ the\ model} \quad (1)$$

From the calculations carried out, shear, compression and torsion stress in the bell tower walls were found to be negligible. This was true for any direction of the seismic waves contained within the tangents drawn from the building to the isoseismal line of maximum intensity (Figure 9). As a result of this, flexural tensile was adopted in order to obtain the acceleration causing cracking in equation 1.

The final result obtained was a peak acceleration in the range **0.10g - 0.13g**, to cause cracking of the lower wall (Figure 7, view 1), in the Restábal Church bell tower (Figure 10).

Ground Acceleration

Figure 5 shows the data for the minimum peak acceleration, being the cause of liquefaction in each one of the studied sites, and the minimum value in the peak acceleration that fissured the Restábal Church bell tower.

The different curves for acceleration versus epicentral distance were adjusted to the above five values by means of the non-linear regression method (Figure 11). The adjustment was carried out with the help of the computer program Mathematica [22]. Equation 2 plotted in Figure 10 (curve 1), is the curve with the best adjustment (Chi Squared value of 0.0005466).

$$\log A = 0.61128 - 1.07539 \log(D+5.84741) + \log(0.00067D) \quad (2)$$

This curve does not represent a relation for the attenuation of acceleration with distance to the epicentre, due to the limited data used in its determination. It could be considered as a limiting curve, above which the acceleration values of those sites studied are most likely to be found. In the same figure, two curves have been drawn to show the peak acceleration's attenuation with distance for an earthquake of magnitude 6.6. Curve 2 represents Campbell's curve [4], and curve 3 represents the Fukushima and Tanaka curve [8]; they indicate a possible upper limit to the peak acceleration.

SUMMARY

Fieldwork and techniques used in this research have allowed us to develop a method for the calculation of a lower limit for the peak acceleration in the case of historic earthquakes, in sites where, either ground liquefaction or moderate cracking of the buildings effected by the earthquake took place.

REFERENCES

1 Atkinson, R. H., Amadei, B. P., Saeb, S. and Sure S. 1989. Response of Masonry Bed Joints in Direct Shear. *Journal of Structural Engineering* 115(9):2276-2296.

2 Benedetti, D., and Benzoni, G.M. 1984. A numerical model for seismic analysis of masonry buildings. Experimental correlations. *Earthquake Engineering Structural Dynamics* 12:817-831.

3 Benedetti, D., Modena, C. and Vescovi, U. 1978. Ricerca sperimentale sui parametri di resistenza e deformabilitá di murature in laterizio armato e alveolato. *Construire* 109:1-16.

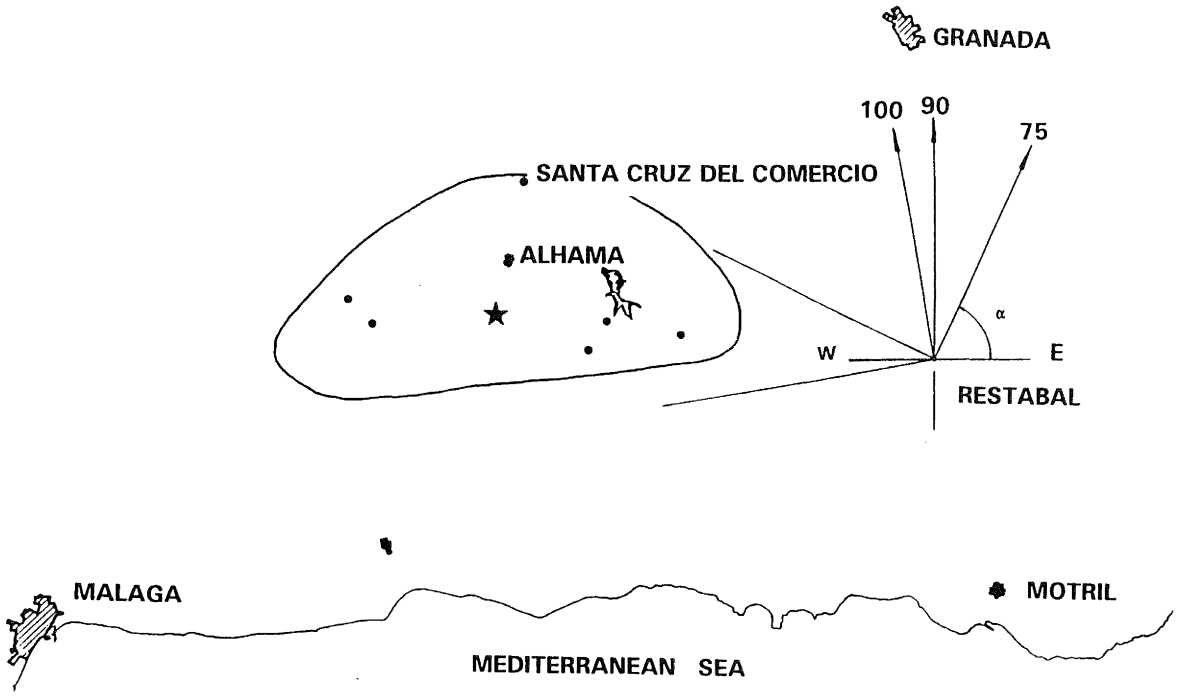

FIGURE 9 Range of possible arrival directions for seismic waves S in Restábal.

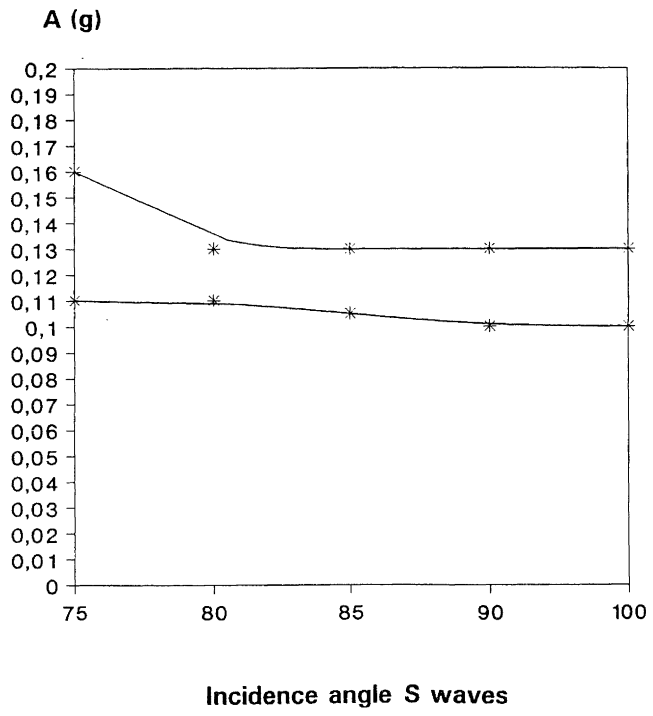

FIGURE 10 ***Peak acceleration causing the cracking versus incidence angle S waves in the most cracked wall (Figure 7, wall 1), in the Restábal church bell tower.***

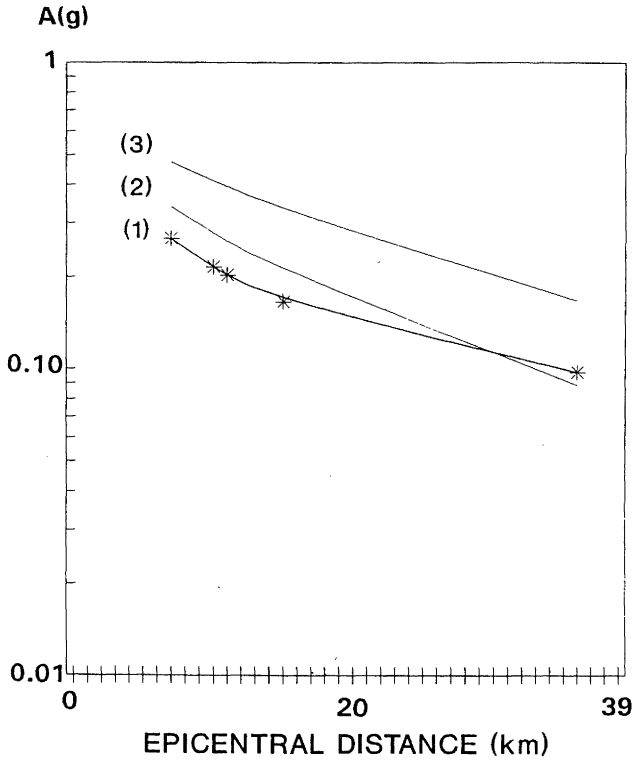

FIGURE 11 ***Curve 1 represents the minimum values in the peak acceleration of four sites studied versus epicentral distance. Curves 2 and 3 represent attenuation curves of Campbell [1981] and Fukushima and Tanaka [1990].***

4 Campbell, K.W. 1986. Near-source attenuation of peak horizontal acceleration. *Bulletin of the Seismological Society of America* 71:2039-2070.

5 Commission of the European Communities 1989. *Eurocode No. 6 draft. Common unified rules for masonry structures*, Brussels.

6 Fernández de Castro, M., Lasala, L.P., Cortázar, D. y Gonzalo J. 1885. *Terremoto de Andalucía. Informe de la comisión española nombrada para su estudio dando cuenta del estado de los trabajos en marzo de 1885*, Imprenta M. Tello, Madrid.

7 Fouqué, F. 1884. Mission d´Andalouise: Etudes relatives au tremblement de terre du 25 décembre 1884, et à la constitution géologique du sol ébranté par les secousses. *Academie Sciences, Memoires* Vol. XIX, Paris

8 Fukushima, Y., and Tanaka T. 1990. A new attenuation relation of peak horizontal acceleration of strong earthquake ground motion in Japan. *Bulletin of Seismological Society of America* 80:757-783.

9 Ghobarah A. and Baumber T. 1992. Seismic response and retrofit of industrial brick masonry chimneys. *Canadian Journal of Civil Engineering* 19:117-128.

10 López, A., Martín, A., and Mézcua J. 1980. *Terremoto de Andalucía: Influencia en sus efectos de las condiciones del terreno y del tipo de construcción. El terremoto de Andalucía del 25 de diciembre de 1884*, Instituto Geográfico Nacional, Madrid.

11 Muñoz, D., and Udías A. 1980. *Estudio de los parámetros y series de réplicas del terremoto de Andalucía del 25 de diciembre de 1884 y de la sismicidad de la región Granada-Málaga. El terremoto de Andalucía del 25 de diciembre de 1884*. Instituto Geográfico Nacional, Madrid.

12 Muñoz, D., and Udías, A. 1991. *Three large historical earthquake in southern Spain. Seismicity, Seismotectonics and Seismic risk of the Ibero-Marghebian region*. Instituto Geográfico Nacional, Madrid.

13 Page A. W. 1978. Finite Element Model for Masonry. *Journal of Structural Division*. Proc. A.S.C.E. 104(ST8):1267-1285.

14 Rodriguez, J. 1984. *Curso Aplicado de Cimentaciones, Colegio de Arquitectos*, Madrid.

15 Seed, H., and Idriss, I. 1982. *Ground Motions and Soil Liquefaction during Earthquakes*. Earthquake Engineering Research Institute, Berkeley, C.A.

16 State Capital Construction Commission 1974. *Earthquake-Resistant Design Code for Industrial and Civil Buildings*. Building Publishing House, Pekin, China.

17 Tarramelli, T., Mercalli, G. 1885. I terremoti Andalucí cominciati il 25 decembre 1884. *Reale Accademi di Lincei*, Vol. CCLXXXIII, Roma.

18 Tomazevic, M., Velechovsky, T., and Weiss, P. 1992. The effect of interventions in the floor structural system on the seismic resistance of historic stone masonry buildings. An experimental study. *Proc. Tenth World Conference on Earthquake Engineering*, Madrid 9:5321-5326

19 Turnsek, V., and Cacovic, F. 1970. Some experimental results on strength of brick-masonry walls. *Proc. 2nd International Brick-Masonry Conference, Stoke-on-Trent* 149-156.

20 Vanelli, F., and Benassi, F. 1983. *Penetrómetro dinámico Sunda DL030*. Studio de geología e meccanica di terreni, Bolonia, Italia.

21 Wilson, E.L. 1984. *Structural Analysis Programs. A Series of Computer Programs for the Static and Dynamic Finite Element Analysis of Structures*. Computers and Structures Inc., Berkeley, C.A.

22 Wolfram, E. 1992. *Mathematica. A System for Doing Mathematics by Computer.* Addison-Wesley Publishing Company Inc. N.Y.

23 Yokel, F.Y., and Dikkers, R.D. 1971. Strength of load bearing masonry walls. *Journal of Structural Division.* Proc. A.S.C.E. (ST5):1593-1609.

24 Zhou, S.G. 1981. Influence of fine on evaluating liquefaction of sand by the S.P.T. *Proc. Int. Conf. on Recent Advances in Geotechnical Earthquakes Engineering and Soil Dynamics*, St Louis 2:167-172.

LIST OF SYMBOLS

A	- peak ground acceleration
a_{min}	- minimum liquefaction acceleration
b	- distribution factor of shear stresses
D	- epicentral distance
d_s	- depth of sand layer
d_w	- depth of water table
f_t	- tensile strength
g	- acceleration of gravity
H	- depth of layer of soil
I	- Modified Mercalli Intensity
S.P.T.	- standard penetration resistance
N_{crit}	- critical value of S.P.T.
N_1	- modified S.P.T.
r	- proportionality ratio of tensions
r_d	- shear stress reduction coefficient
W.T.	- water table
ρ	- density
τ	- shear stress induced by the earthquake
τ_u	- average shear stress on the horizontal cross-sectio
σ	- total overburden pressure
σ'	- effective overburden pressure
σ_0	- average compressive stress